International Journal of Heat and Mass Transfer 52 (2009) 3070–3078

Contents lists available at ScienceDirect

International Journal of Heat and Mass Transfer

journal homepage: www.elsevier.com/locate/ijhmt

Heat transfer in a conical cylinder with porous medium

N.J. Salman Ahmed [a], Irfan Anjum Badruddin [b,*], Z.A. Zainal [a], H.M.T. Khaleed [a], Jeevan Kanesan [c]

[a] School of Mechanical Engineering, University Sains Malaysia, 14300 Nibong Tebal, Malaysia
[b] Department of Mechanical Engineering, University of Malaya, Kuala Lumpur, Malaysia
[c] Department of Electrical Engineering, University of Malaya, Kuala Lumpur, Malaysia

ARTICLE INFO

Article history:
Received 22 February 2008
Received in revised form 18 November 2008
Accepted 24 December 2008
Available online 21 March 2009

Keywords:
Porous media
Conical cylinder
Natural convection
Radiation
Cone angle
FEM

ABSTRACT

In this paper, numerical study of heat transfer in a conical annular cylinder fixed with saturated porous medium is presented. The heat transfer is assumed to take place by natural convection and radiation. The inner surface of conical cylinder is maintained at uniform wall temperature. The governing partial differential equations are non-dimensionalised using suitable non-dimensional parameters and then solved by using finite element method. The porous medium is divided using triangular elements with uneven element size. A computer software is used to solve the coupled momentum and energy equations in an iterative manner. The results are discussed for various values of geometric and physical parameters of porous medium with emphasis on cone angle of the cylinder. It is seen that the cone angle plays a vital role in heat transfer from the hot surface to porous medium.

1. Introduction

The heat transfer and other phenomena in porous media have become hot topics of research during the last few years, which is reflected in number of articles being published, addressing various problems related to porous medium. The research efforts directed towards porous medium is justified by the fact that it is used in various applications covering a wide range of engineering and science disciplines such as geophysics, petroleum engineering, oil recovery techniques, thermal insulation of building, cooling of nuclear reactors, heat exchangers etc. The research work focusing different aspects of porous medium has been well documented. Recent books by Nield and Bejan [1] Vafai [2,3] Pop and Ingham [4] provide a good understanding of the subject and also give the clear picture of research work being carried out in this field. Nath and Satyamurthy [5] have used finite difference method to investigate free convection heat transfer in an annular cylinder filled with porous medium. Prasad and Kulacki [6] have analyzed the natural convection in a vertical porous annulus. They found that the local rate of heat transfer is much higher near the top edge of the cold wall. Prasad et al. [7] have carried out experimental investigations of natural convection in a vertical annulus filled with saturated porous medium. Irfan et al. [8] have investigated the effect of radiation and viscous dissipation in an annular porous medium. Yih [9] has studied the effect of radiation on natural convection over a vertical cylinder using finite difference method. Yih [10] also considered a vertical cone embedded in a porous medium to study the boundary layer analysis for uniform lateral mass flux effect on natural convection of non-Newtonian power-law fluids. Ching-Yang Cheng [11] has used an integral approach to investigate heat and mass transfer by natural convection from truncated cones in porous media. Murthy and Singh [12] have studied the thermal dispersion effects over a cone with the help of similarity solution. The analytical solutions for MHD fully developed upward or downward natural-convection velocity and temperature profiles for four boundary conditions in an open-ended vertical concentric porous annuli has been presented by A1-Nimr [13]. Chamkha [14] has considered the steady, laminar, free convection flow along a vertical cone and a wedge immersed in an electrically conducting fluid-saturated porous medium in the presence of a transverse magnetic field. The effect of thermal radiation on the non-Darcy natural convection flow over a vertical cone and wedge embedded in a porous medium with variable viscosity and wall mass flux was analyzed by Al-Harbi [15].

On the other hand, the porous medium fixed with the complex geometry such as an annular cylinder resting over annular cone has not been given attention. Such geometries are used in various types of biomass gasifiers. The present study is focused to investigate the heat transfer in a porous medium fixed within an annulus resting on an annular cone.

2. Analysis

Consider the porous medium fixed within an annular conical cylinder as shown in Fig. 1. The conical cylinder has an inner and

* Corresponding author. Tel.: +603 79674463; fax: +603 79675317.
E-mail address: Irfan_magami@Rediffmail.com (I.A. Badruddin).

0017-9310/$ - see front matter © 2009 Elsevier Ltd. All rights reserved.
doi:10.1016/j.ijheatmasstransfer.2008.12.030

Nomenclature

A_r	aspect ratio = H/L
c_p	specific heat (J/kg °C)
g	gravitational acceleration (m/s^2)
H	height of cylindrical portion of geometry (m)
h	height of the conical portion of geometry (m)
k	thermal conductivity (W/m °C)
K	permeability of the porous medium (m^2)
L	$= r_o - r_i$ (m)
$\overline{N}u$	average Nusselt number respectively
q_r	radiation flux (W/m^2)
r, z	cylindrical co-ordinates (m)
$\bar{r}, \bar{z}$	non-dimensional co-ordinates
R_r	radius ratio = $r_o - r_i/r_i$
Ra	Rayleigh number
R_d	radiation parameter
$T, \overline{T}$	dimensional (°C) and non-dimensional temperature respectively
u, w	velocity in r and z directions (m/s)

Greek symbols

α	thermal diffusivity (m^2/s)
β	coefficient of thermal expansion (1/°C)
β_R	absorption coefficient (1/m)
θ	cone angle = $\tan^{-1}$(L/h)
ρ	density (kg/m^3)
ν	coefficient of kinematic viscosity
σ	Stephan Boltzmann constant
ψ	stream function
$\overline{\psi}$	non-dimensional stream function

Subscripts

h	hot
∞	conditions at outer radius
i	inner
o	outer

outer radius as r_i and r_o respectively. The angle θ is measured between the hot and cold surface at the lower corner of the cone. The r and z axis indicate the radial and vertical direction of the geometry being considered. The inner surface of conical cylinder is maintained at isothermal temperature T_h and the surface along the outer radius is set to T_∞. The upper surface of conical cylinder is adiabatic.

The following assumptions are applied to the problem under consideration.

- Porous medium is saturated with fluid.
- The fluid is assumed to be gray emitting and absorbing but non-scattering.
- The fluid and medium are in local thermal equilibrium everywhere.
- The porous medium is isotropic and homogeneous.
- Fluid properties are constant except the variation of density.

For the problem under consideration, the equations governing the heat and fluid flow inside the porous medium can be given as:

$$\frac{\partial(ru)}{\partial r} + \frac{\partial(rw)}{\partial z} = 0 \tag{1}$$

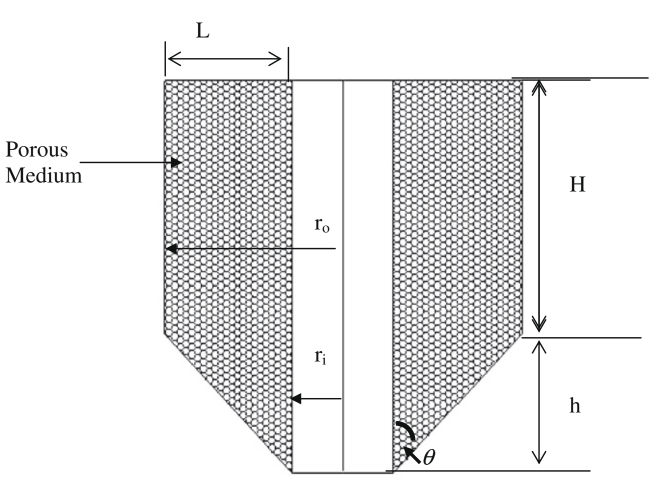

Fig. 1. Conical cylinder filled with porous medium.

Velocity in radial and vertical direction is:

$$u = \frac{-K}{\mu}\frac{\partial p}{\partial r}, \quad w = \frac{-K}{\mu}\left(\frac{\partial p}{\partial z} + \rho g\right) \tag{2a}$$

Invoking Boussinesq approximation as:

$$\rho = \rho_\infty[1 - \beta(T - T_\infty)] \tag{2b}$$

Mathematical operation on Eqs. (2a) and (2b) results as:

$$\frac{\partial w}{\partial r} - \frac{\partial u}{\partial z} = \frac{gK\beta}{\nu}\frac{\partial T}{\partial r} \tag{2c}$$

Energy equation is given as:

$$u\frac{\partial T}{\partial r} + w\frac{\partial T}{\partial z} = \alpha\left(\frac{1}{r}\frac{\partial}{\partial r}\left(r\frac{\partial T}{\partial r}\right) + \frac{\partial^2 T}{\partial z^2}\right) - \frac{1}{\rho c_p}\left(\frac{1}{r}\frac{\partial}{\partial r}(rq_r) + \frac{\partial q}{\partial z}\right) \tag{3}$$

The continuity Eq. (1) can be satisfied by introducing the stream function ψ as:

$$u = -\frac{1}{r}\frac{\partial\psi}{\partial z}, \quad w = \frac{1}{r}\frac{\partial\psi}{\partial r} \tag{4}$$

The boundary conditions are:

$$\text{at } 0 \le z \le (H+h) \ \ \& \, r = r_i, \ \ T = T_h, \ \ u = 0, \ \ w = 0 \tag{5a}$$

$$\text{at } 0.001 \le z \le (H+h) \ \ \& \, r = r_o, \ \ T = T_\infty, \ \ u = 0, \ \ w = 0 \tag{5b}$$

Invoking Rosseland approximation for radiation

$$q_r = -\frac{4\sigma}{3\beta_R}\frac{\partial T^4}{\partial r} \tag{6}$$

Expanding T^4 about T_∞ using Taylor series and neglecting higher order terms [16] results:

$$T^4 \approx 4TT_\infty^3 - 3T_\infty^4 \tag{7}$$

The following non-dimensional variables are used:

$$\bar{r} = \frac{r}{L}, \quad \bar{z} = \frac{z}{L}, \quad \overline{\psi} = \frac{\psi}{\alpha L}, \quad \overline{T} = \frac{(T - T_\infty)}{(T_w - T_\infty)}, \\ R_d = \frac{4\sigma T_\infty^3}{\beta_{Rk}}, \quad Ra = \frac{g\beta_T \Delta TKL}{\nu\alpha}. \tag{8}$$

After substituting the above non-dimensional parameters, Eqs. (3) and (6) take the form:

$$\frac{\partial^2\overline{\psi}}{\partial\bar{z}^2}+\bar{r}\frac{\partial}{\partial\bar{r}}\left(\frac{1}{\bar{r}}\frac{\partial\overline{\psi}}{\partial\bar{r}}\right)=\bar{r}Ra\frac{\partial\overline{T}}{\partial\bar{r}} \quad (9)$$

$$\frac{1}{\bar{r}}\left[\frac{\partial\overline{\psi}}{\partial\bar{r}}\frac{\partial\overline{T}}{\partial\bar{z}}-\frac{\partial\overline{\psi}}{\partial\bar{z}}\frac{\partial\overline{T}}{\partial\bar{r}}\right]=\left(1+\frac{4R_d}{3}\right)\left(\frac{1}{\bar{r}}\frac{\partial}{\partial\bar{r}}\left(\bar{r}\frac{\partial\overline{T}}{\partial\bar{r}}\right)+\frac{\partial^2\overline{T}}{\partial\bar{z}^2}\right) \quad (10)$$

The corresponding boundary conditions are:

$$\text{at } 0\le\bar{z}\le\frac{H+h}{L} \quad \& \quad \bar{r}=\bar{r}_i,\quad \overline{T}=1,\quad \overline{\psi}=0 \quad (11a)$$

$$\text{at } \frac{0.001}{L}\le\bar{z}\le\frac{H+h}{L} \quad \& \quad \bar{r}=\bar{r}_o,\quad \overline{T}=0,\quad \overline{\psi}=0 \quad (11b)$$

2.1. Numerical method

Eqs. (2a) and (2b) are coupled partial differential equations to be solved in order to predict the heat transfer behavior. In the present work, finite element method is employed to get the solution of above mentioned coupled equations. A simple 3 nodded triangular element is used to descritise the porous medium. The solution variables $\overline{T}$ and $\overline{\psi}$ vary linearly inside the element and can be expressed as:

$$\overline{T}=N_1\overline{T}_1+N_2\overline{T}_2+N_3\overline{T}_3 \quad (12a)$$

$$\overline{\psi}=N_1\overline{\psi}_1+N_2\overline{\psi}_2+N_3\overline{\psi}_3 \quad (12b)$$

where N_1, N_2, N_3 are shape functions. Integrating Eqs. (2a) and (2b) using Galerkin method yields two coupled matrix form of equations. Details of FEM can be obtained from [17,18] These coupled matrix equations for an element is assembled to get the global matrix equation for the whole domain, which is solved iteratively to obtain $\overline{T}$ and $\overline{\psi}$ in the porous medium. In order to get accurate results, tolerance level of solution for $\overline{T}$ and $\overline{\psi}$ are set at 10^{-5} and 10^{-9} respectively. The tolerance level indicates the difference between previous iteration and current iteration

Table 1
$\overline{Nu}$ comparison to validate present method.

Aspect ratio	Nath and Satyamurthy [5]	Prasad and Kulacki [6]	Rajamani et al. [19]	Present
3	3.81	3.70	3.868	3.8038
5	3.03	3.00	3.025	2.9830
8	2.45	2.35	2.403	2.3749

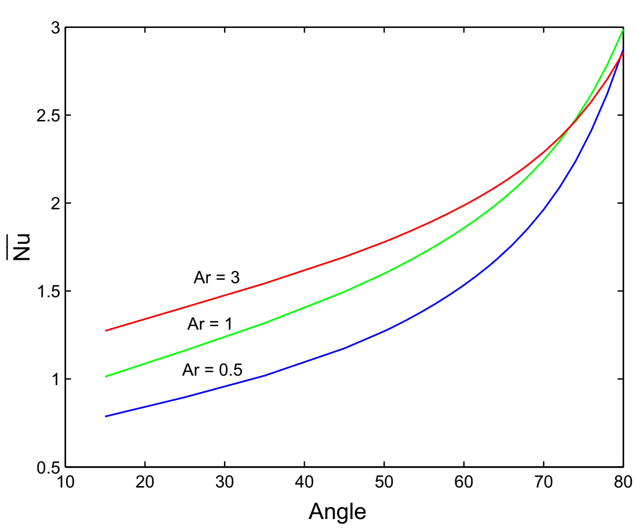

Fig. 2. Average Nusselt number variation with cone angle and aspect ratio.

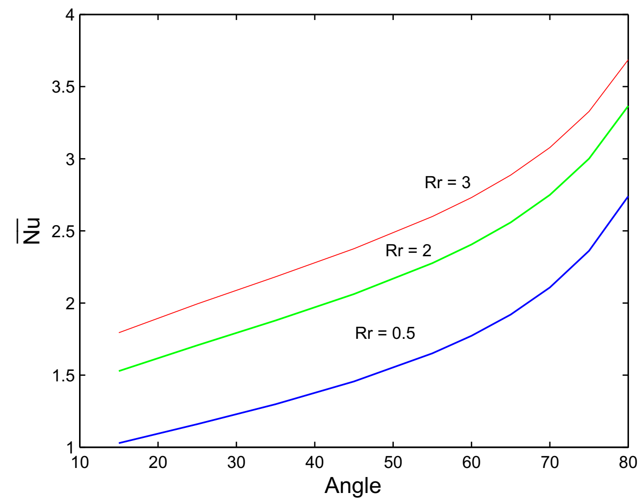

Fig. 3. Average Nusselt number variation with cone angle and radius ratio.

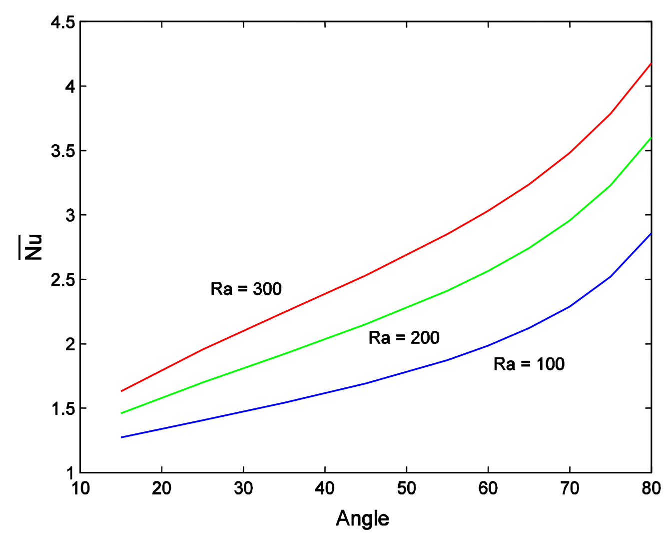

Fig. 4. Average Nusselt number variation with cone angle and Rayleigh number.

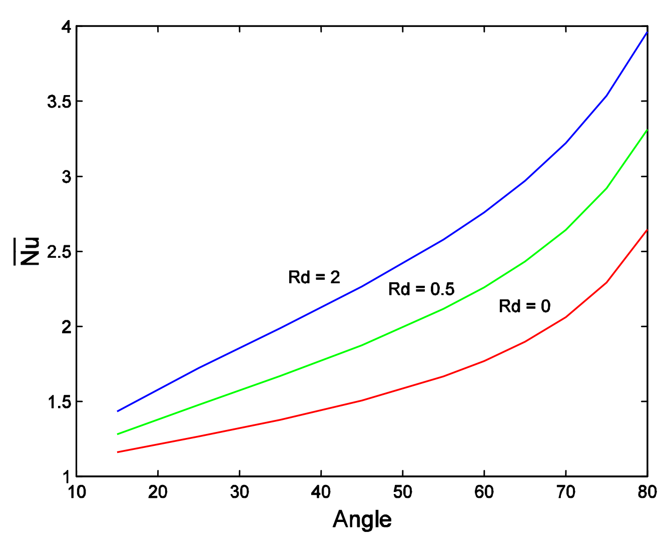

Fig. 5. Average Nusselt number variation with cone angle and Radiation parameter.

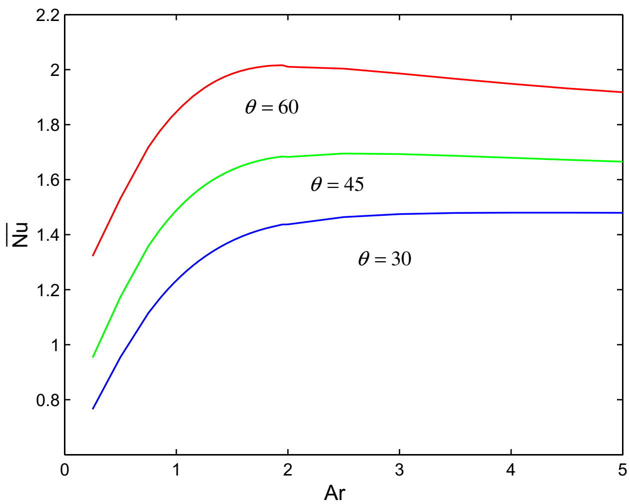

Fig. 6. Average Nusselt number variation with aspect ratio.

for a variable at all nodes. Fine mesh is used in the areas where large variations in solution variables $\overline{T}$ and $\overline{\psi}$ are expected. While meshing the domain, it is taken care that the mesh size does not influence the solution. A mesh independent study is carried out and then a mesh size of 3024 elements is selected. The computations are carried out on a high end computer. The results are presented in terms of average Nusselt number at the hot surface of the annular conical cylinder, with respect to various parameters such as the angle of cone θ, aspect ratio H/L, radius ratio $(r_o - r_i)/r_i$ radiation parameter and Rayleigh number. The average Nusselt number is defined as

$$\overline{Nu} = -\frac{\int_0^{\bar{z}} \left(1 + \frac{4R_d}{3}\right) \frac{\partial \overline{T}}{\partial \bar{r}}\Big|_{\bar{r}=\bar{r}_i}}{\bar{z}} \tag{13}$$

The present methodology is verified by comparing the results with those of earlier published data. In order to make a common platform for comparison, the present problem is reduced to a porous medium fixed in an annulus. This is done due to unavailability of data for the geometry being considered in the present work. Table 1 shows the comparison between present results and those published earlier [5,6,19]. It is obvious from Table 1. that the present method has good agreements with the previous results and thus encourages to further predict the behavior of heat and fluid flow inside the porous medium fixed within an annular conical cylinder.

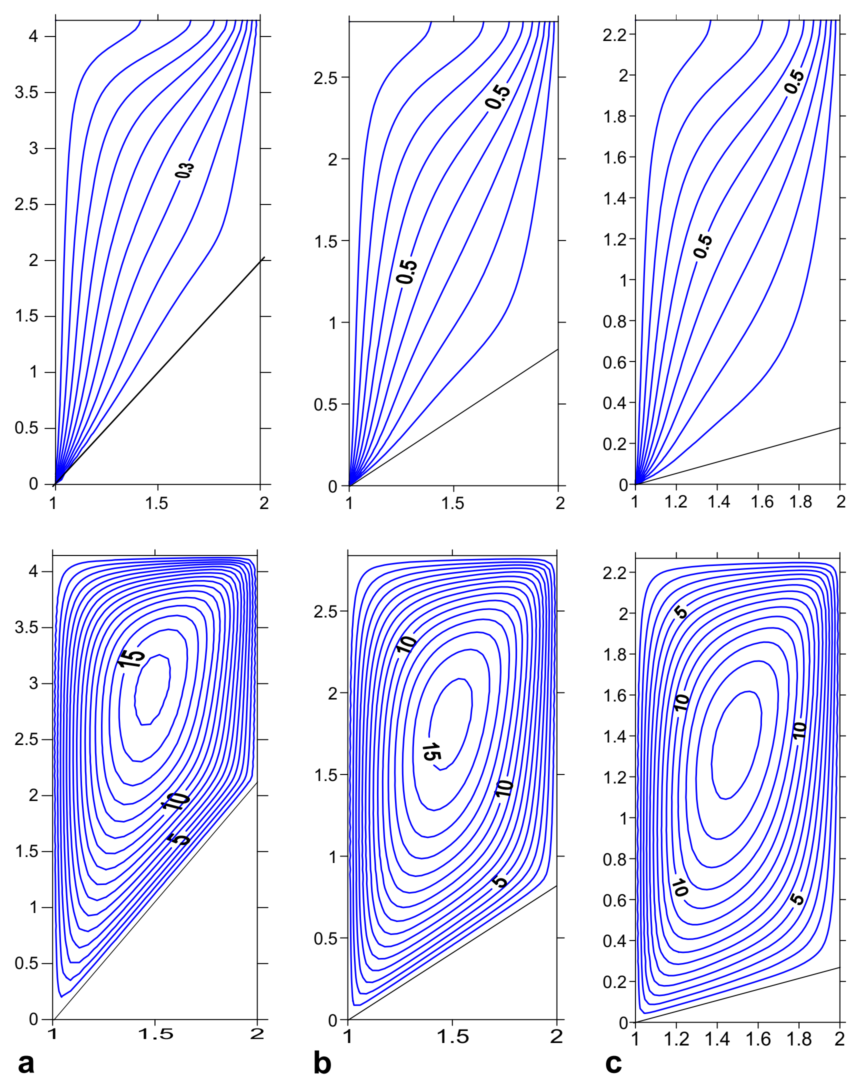

Fig. 7. Isotherms and streamlines for different values of cone angle (a) $\theta = 25$, (b) $\theta = 50$, (c) $\theta = 75$.

3. Results and discussion

Fig. 2 shows the average Nusselt number variation with the angle of conical cylinder corresponding to three values of aspect ratio, 0.5, 1 and 3.The other parameters being $Ra = 100$, $Rd = 1$ and $Rr = 1$. As obvious from the figure, the average Nusselt number increases with increase of angle of the conical cylinder. The average Nusselt number increases with increase in the aspect ratio of the cylindrical portion of the conical cylinder. At higher cone angle, the Nusselt number variations with respect to change in the aspect ratio are marginal.

Fig. 3 shows the average Nusselt number variation with respect to different values of radius ratio of the conical cylinder. The radius ratio is the ratio of width of the porous medium inside the cylinder, to the inner radius of cylinder. Fig. 3 shows Nusselt number values corresponding to radius ratio 0.5, 2 and 3. The other parameters being $Ar = 2$, $Ra = 500$, $Rd = 3$. It can be seen from Fig. 3 that the average Nusselt number increases with the increase in angle as well as the radius ratio of the conical cylinder.

Fig. 4 shows the average Nusselt number variations with respect to cone angle and Rayleigh number. The figure corresponds to $Ar = 2$, $Rd = 1$ and $Rr = 1$. As expected, the average Nusselt number increases with increase in the Rayleigh number. It can be inferred from the figure that, the effect of cone angle is stronger at higher values of Rayleigh number thus the line corresponding to $Ra = 300$ is steeper than the line corresponding to $Ra = 100$. Fig. 5 reflects the variations of average Nusselt number behavior with respect to cone angle and the radiation parameter. This figure corresponds to the values $Ar = 2$, $Ra = 100$, $Rr = 1$ As seen in the Fig. 5, the average Nusselt number increases with increase in the radiation parameter.

Fig. 6 demonstrates the average Nusselt number variations with respect to aspect ratio of the cylinder. The figure is obtained for three different values of cone angle 30°, 45° and 60°. The other constant parameters for Fig. 6 are $Rd = 1$, $Ra = 100$ and $Rr = 1$. The average Nusselt number increases with increase in aspect ratio Ar, and then decreases marginally with subsequent increase in the aspect ratio of cylindrical portion. The variation in Nusselt number beyond certain value of Ar is unnoticeable. It can be recalled here that, in an annular porous cylinder, the average Nusselt number first increases, reaches a maximum value at an aspect ratio around 1 and then declines. The decline of Nusselt number in an annular porous medium is quite noticeable, which is not observed in the present case (conical cylinder) especially for cone angle less than

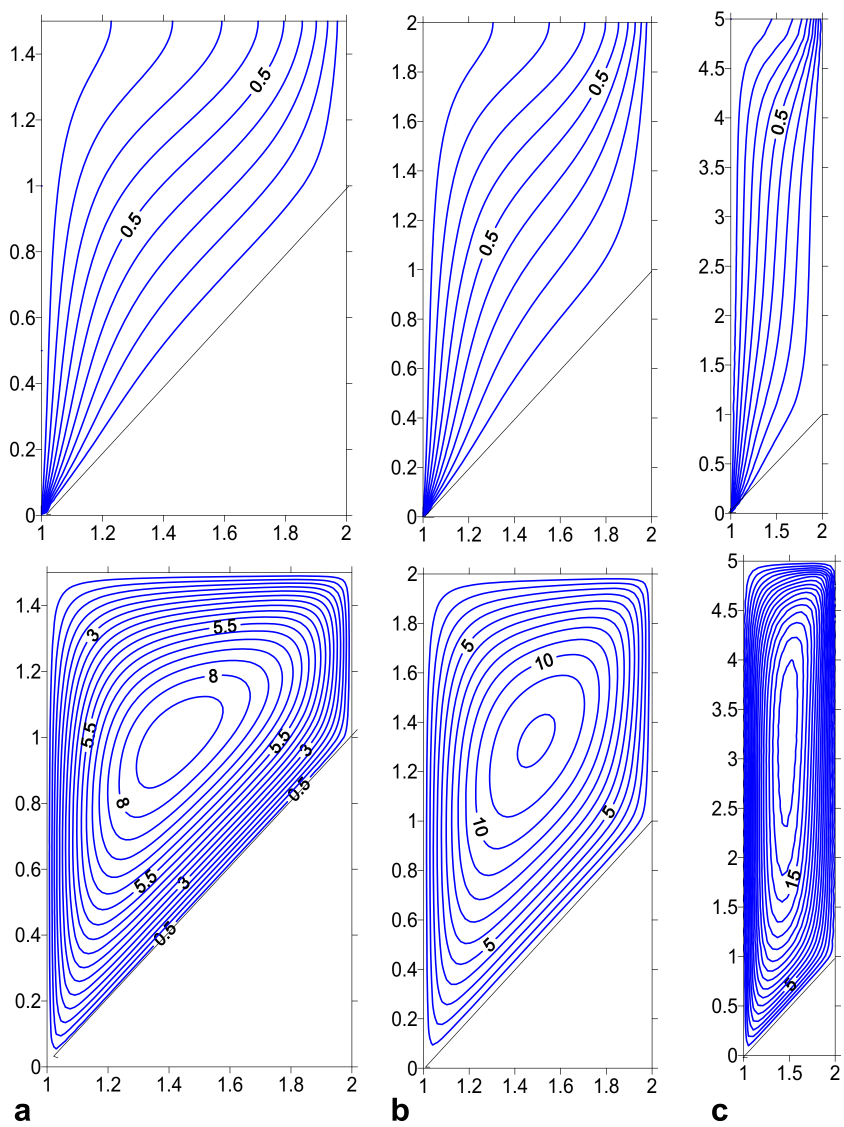

Fig. 8. Isotherms and streamlines for different values of aspect ratio (a) $Ar = 0.5$, (b) $Ar = 1$, (c) $Ar = 4$.

60°. It is also observed though not noticeable in Fig. 6 that, if the cone angle is increased then the marginal decline of average Nusselt number begins at lower aspect ratio. For instance at $\theta = 45°$, the decline of average Nusselt number begins at $Ar > 3$, however for $\theta = 60°$, the Nusselt number starts decreasing at $Ar > 1.9$.

Fig. 7 shows the isotherms and streamlines for different values of cone angle. This figure corresponds to $Rd = 1$, $Ra = 100$, $Rr = 1$ and $Ar = 2$. It is obvious from the figure that the isotherms move towards the hot surface as angle of the cone increases. This indicates that the heat transfer from hot surface of the conical cylinder to the porous medium increases with increase in the cone angle. It is also clear from isotherms that the temperature gradient at the hot surface goes on decreasing as the height of the cylinder increase. The temperature gradient at upper hot surface is substantially low since the isothermal line moves away from the hot surface thus indicating that the heat transfer is low in this region compared to the lower portion of the conical cylinder. The movement of the fluid is indicated by streamlines. The fluid moves upward towards the hot surface and flows across the porous medium then falls towards the cold surface of the cylinder to complete the cycle. The circular cell of the fluid movement is concentrated at the upper half of the cylinder for low cone angle, but it moves downwards as the angle of the cone increases. It is also observable from the figure that the circular cell of fluid movement changes its angle of orientation as the angle of cone changes. At lower cone angle, the cell is oriented almost towards the upper right and lower left corner of the cylinder. As the angle of cone increases the cell orientation turns parallel to the vertical cylinder.

Fig. 8 reflects the isothermal lines and streamlines variations with respect to aspect ratio of the cylindrical portion of the conical cylinder. The figure is obtained for three values of aspect ratio i.e. $Ar = 0.5$, 1 & 4 corresponding to $Rd = 1$, $Ra = 100$, $Rr = 1$ and $\theta = 45$. The isothermal lines reveal that the increase in the aspect ratio leads to crowding of isothermal lines at lower left and upper right

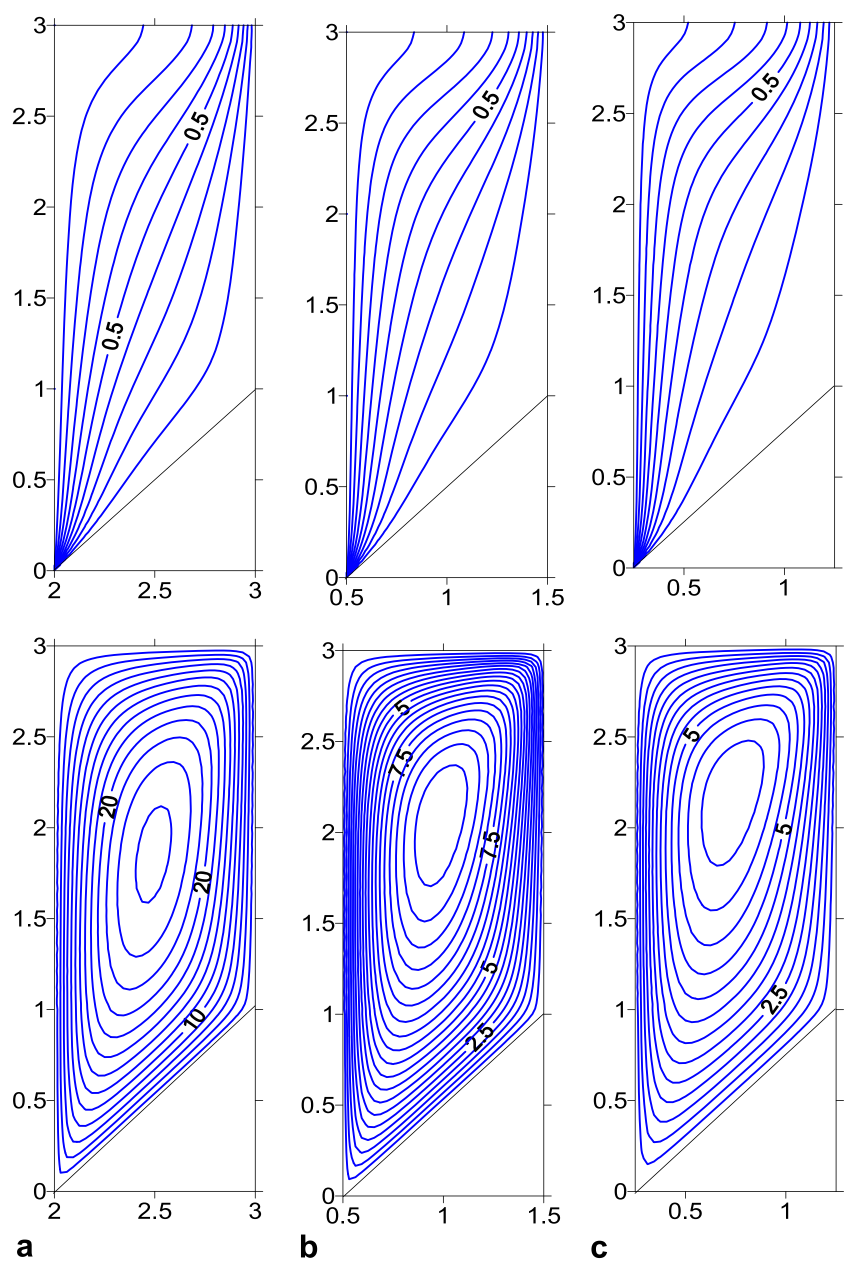

Fig. 9. Isotherms and streamlines for different values of radius ratio (a) $Rr = 0.5$, (b) $Rr = 2$, (c) $Rr = 4$.

corner of the conical cylinder. There is continuous variation in the temperature gradient for major portion of hot surface at lower aspect ratio (Fig. 8a) indicating that the heat transfer rate continuously varies along the height of the cylinder which is not the case at higher aspect ratio (Fig. 8c). The fluid circulation changes orientation as the aspect ratio increases.

Fig. 9 shows the isothermal lines and streamlines for various values of radius ratio. This figure corresponds to the values $Rd = 1$, $Ra = 100$, $Ar = 2$ and $\theta = 45$. It can be seen from Fig. 9 that the isothermal lines move towards the hot surface. It is observable that the penetration of heat into the depth of porous medium reduces with increase in the radius ratio. The fluid circulation centre shifts towards upper half of the cylinder when radius ratio increases.

Fig. 10 reveals the streamline and isothermal line behavior with respect to Rayleigh number. This figure is obtained for $Ra = 100$, 500 & 1000 at $Rd = 5$, $Rr = 1$, $Ar = 2$, $\theta = 45$. The heat transfer rate increases substantially with increase in Rayleigh number which is clearly observable in Fig. 10. The isothermal lines gets distorted and crowded near lower left corner and upper right corner of the cylinder showing an increase in the heat transfer in these areas of conical cylinder. It is also notable that the distortion of isothermal lines occurs in the conical portion of the cylinder. The fluid orientation turns towards the upper right and lower left corner of the conical cylinder when Rayleigh number is increased. As obvious from streamlines, the fluid velocity increases with increase in the Rayleigh number. Fig. 11 demonstrates the effect of radiation parameter on the streamlines and isothermal lines. This figure is obtained for $Ra = 100$, $Rr = 1$, $Ar = 2$, $\theta = 45$. Fig. 11a corresponds to natural convection when radiation effect is absent. The distortion of isotherms decrease with increase in the radiation parameter.

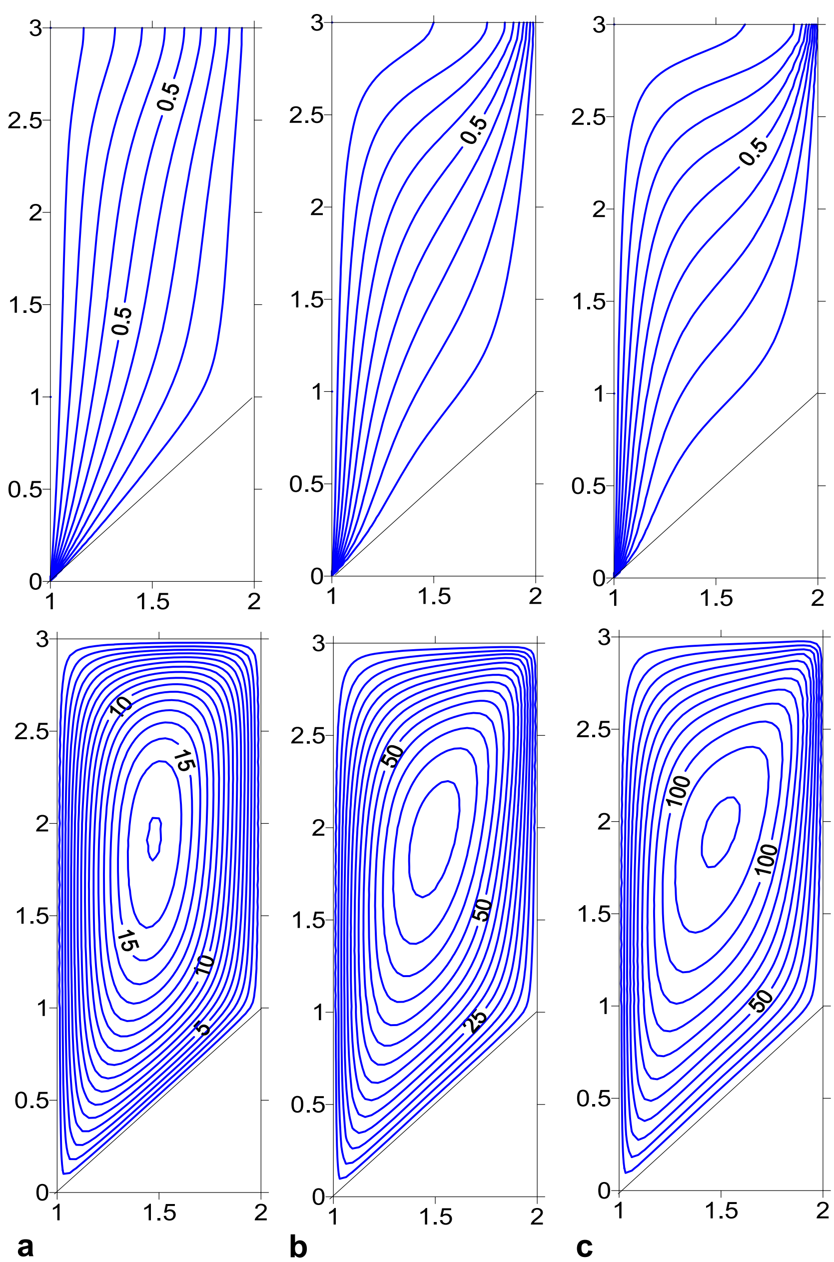

Fig. 10. Isotherms and streamlines for different values of Rayleigh number (a) $Ra = 100$, (b) $Ra = 500$, (c) $Ra = 1000$.

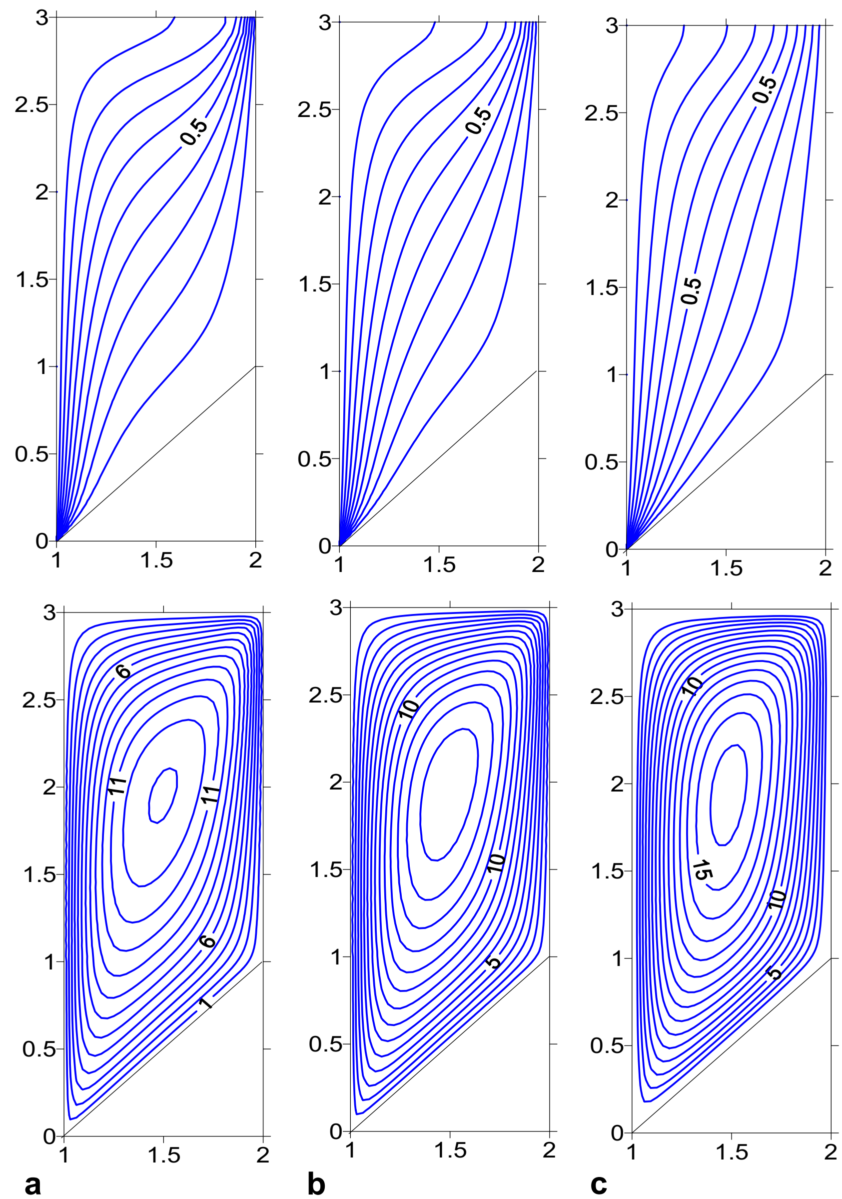

Fig. 11. Isotherms and streamlines for different values of Radiation parameter (a) $Rd = 0$, (b) $Rd = 0.5$, (c) $Rd = 2$.

4. Conclusion

The present study investigates the heat transfer behavior inside a porous medium fixed within a complex geometry with cone and cylinder merged together. Finite element method is used to solve the complex partial differential equations. The results indicate that the cone angle of the conical cylinder has strong influence on average Nusselt number. The average Nusselt number increases with increase in the cone angle. It is seen that the average Nusselt number increases sharply at higher values of cone angle. The average Nusselt number increases with increase in aspect ratio until certain value of *Ar* and then remains almost constant at lower cone angle. The isothermal lines move towards the hot surface as angle of the cone increases which leads to increased heat transfer rate. The circular cell of the fluid concentrates at the upper half of the cylinder for low cone angle, but it moves downwards as the angle of the cone increases.

References

[1] D.A. Nield, A. Bejan, Convection in Porous Media, second ed., Springer-Verlag, New York, 1999.

[2] K. Vafai, Hand Book of Porous Media, Marcel Dekker, New York, 2000.

[3] K. Vafai, Handbook of Porous Media, second ed., Taylor & Francis Group, Boca Raton, 2005.

[4] I. Pop, D.B. Ingham, Convective heat transfer: mathematical and computational modeling of viscous fluids and porous media, Pergamon, Oxford, 2001.

[5] S.K. Nath, V.V. Satyamurthy, 1985. Effect of aspect ratio and radius ratio on free convection heat transfer in a cylindrical annulus filled with porous media, in: Proc. HMT C16-85, 8th Nat. Heat Mass Transfer Conf., India, pp. 189–193.

[6] V. Prasad, F.A. Kulacki, Natural convection in a vertical porous annulus, Int. J. Heat Mass Transfer 27 (2) (1984) 207–219.

[7] V. Prasad, F.A. Kulacki, A.V. Kulkarni, Free convection in a vertical, porous annulus with constant heat flux on the inner wall-experimental results, Int. J. Heat Mass Transfer 29 (5) (1986) 713–723.

[8] Irfan Anjum Badruddin, Z.A. Zainal, Zahid A. Khan, Zulquernain Mallick, Effect of viscous dissipation and radiation in a porous medium embedded within vertical annulus, Int. J. Thermal Sci. 46 (2007) 221–227.

[9] K.A. Yih, Radiation effect on natural convection over a vertical cylinder embedded in a porous media, Int. Comm. Heat Mass Transfer 26 (1999) 1025–1035.

[10] K.A. Yih, Uniform lateral mass flux effect on natural convection of non-Newtonian fluids over a cone in porous media, Int. Comm. Heat Mass Transfer 25 (7) (1998) 959–968.

[11] Ching-Yang Cheng, An integral approach for heat and mass transfer by natural convection from truncated cones in porous media with variable wall temperature and concentration, Int. Comm. Heat Mass Transfer 27 (2000) 537–548.

[12] P.V.S.N. Murthy, P. Singh, thermal dispersion effects on non-Darcy convection over a cone, Comput. Math. Appl. 40 (2000) 1433–1444.
[13] M.A. Al-Nimr, MHD free convection flow in open-ended vertical, concentric porous annuli, Appl. Energy 50 (1995) 293–311.
[14] A.J. Chamkha, Non-Darcy hydromagnetic free convection from a cone and a wedge in porous media, Int. Comm. Heat Mass Transfer 23 (6) (1996) 875–887.
[15] Al- Harbi, Numerical study of natural convection heat transfer with variable viscosity and thermal radiation from a cone and wedge in porous media, Appl. Math. Comput. 170 (2005) 64–75.
[16] A. Raptis, Radiation and free convection flow through a porous medium, Int. Comm. Heat Mass Transfer 25 (1998) 289–295.
[17] L.J. Segerland, Applied Finite Element Analysis, John Wiley and sons, New York, 1982.
[18] R.W. Lewis, P. Nithiarasu, K.N. Seetharamu, Fundamentals of the Finite Element Method for Heat and Fluid Flow, John Wiley and sons, Chichester, 2004.
[19] R.C. Rajamani, C. Srinivas, P. Nithiarasu, K.N. Seetharamu, Convective heat transfer in axisymmetric porous bodies, Int. J. Num. Methods Heat Fluid flow 5 (1995) 829–837.